Electronic Supplementary Information (ESI) for:

Hematite Nanoparticle Clusters with Remarkably High Magnetization Synthesized from Water-Treatment Waste by One-Step "Sharp High-Temperature Dehydration"

L. Yu. Novoselova

Institute of Petroleum Chemistry, Siberian Branch, Russian Academy of Sciences,

4 Academichesky Ave., 634055 Tomsk, Russia

E-mail: novoselova@ipc.tsc.ru

Abbreviations

FTIR	Fourier-transform infrared spectroscopy
HNPCs	hematite nanoparticle clusters
IRP	iron removal precipitate
SHTDH	sharp high-temperature dehydration
TEM	transmission electron microscopy
XRD	X-ray diffraction
XRF	X-ray fluorescence spectroscopy

1.

Iron is the fourth most abundant element in the Earth's crust. Groundwater used around the world for drinking, household, and industrial purposes often has elevated concentrations of iron.[S1–S6] When the iron is removed, large amounts of iron-containing precipitates build up on the equipment of water treatment plants. This precipitate is often regarded as a waste material, and is discharged into the local terrain or sewage system, creating the threat of environmental recontamination.

On a global scale, quite considerable amounts of this waste material are generated; thus, it can be considered as a valuable renewable raw material of anthropogenic origin and used to produce a wide range of useful products.[S7–S9] This idea is both environmentally and economically reasonable and could contribute to sustainable development worldwide.[S10]

2. EXPERIMENTAL

2.1. Materials

Iron removal precipitate (IRP) is a side product of iron removal from groundwater by means of aeration. An IRP sample was taken from the sludge tank of the water treatment system of Tomsk Oblast (Russia). It had a pasty consistency that solidified upon drying, but was easily ground to a powdery state. The sample was dried at room temperature to a constant weight, ground in a porcelain mortar, and then thermally treated to obtain hematite nanoparticle clusters (HNPCs).

2.2. Synthesis of HNPCs

The HNPCs under study were prepared as follows. IRP powder (10 g) was placed in an open quartz test tube and heated with a G3U burner (Kislorod Servis Farm, Russia) (burner flame temperature reaches 1980°C) (**Diagram S1**). The IRP contained a significant amount of water (*vide infra*, **3.2**). Therefore, the sharp, almost instantaneous evaporation of water occurred during the high-temperature treatment of the IRP: the material intensively "seethed" (**for more details, see Section 4**). After the seething subsided, the heat treatment of the material was terminated, and the tube with the resulting powder was cooled under ambient conditions prior to further study.

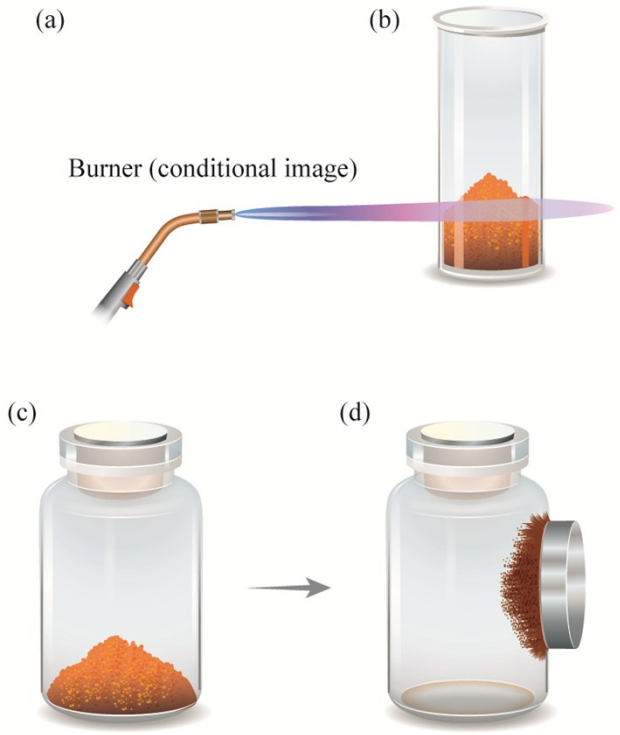

Diagram S1. Schematic representation of the synthesis of HNPCs: (a) burner (schematic image), (b and c) initial IRP material, and (d) resulting HNPCs gathered with a magnet.

Note. The author strongly discourages experiments similar to those described in this manuscript for those who (i) do not have special training for work with burners and (ii) are unfamiliar with how their initial materials would behave during a sharp high-temperature exposure.

3. STRUCTURAL CHARACTERIZATION

3.1. General methods

The nature and size of the particles in the resultant powder were determined through TEM measurements carried out with a Philips CM 12 instrument (Philips, Netherlands) operated at an accelerating voltage of 120 kV and equipped with iTEM software, Ver. 5.1 (Build 1276) (Olympus Soft Imaging Solutions GmbH, Muenster, Germany). The sample was prepared by placing a drop of the powder suspension onto a carbon-coated copper grid, followed by drying in air and transfer to the microscope.

FTIR spectroscopy was performed by the KBr pellet method, using a Nicolet 5700 FTIR spectrometer (Thermo Electron Corporation, United States).

Raman spectra were collected using a Renishaw inVia Basis confocal Raman microscope (ZEISS, Germany) with a 50× lens coupled to a 785-nm laser excitation source. The resolution of this setup was approximately 3 cm^{-1}. To avoid phase changes, which may be induced by the excitation source during collection of the Raman spectra, as previously observed for iron oxides,[S11] the spectra in this study were collected using a low laser power of ~0.8 mW.

The elemental composition of the samples was studied by XRF spectroscopy using a Shimadzu XRF-1800 sequential wavelength dispersive XRF spectrometer (Shimadzu, Japan).

The synthesized HNPCs were characterized with respect to their magnetization with the aid of a pulsed field magnetometer.[S12] The magnetization curve was obtained at 300 K by sweeping the applied magnetic field to 10 kOe.

3.2. Characterization of IRP precursor

Table S1. Elemental composition of IRP

(Quantitative Result)

Analyte	Result	Proc-Calc	Line	Net Int.	BG Int.
Fe	47.3341 %	Quant.-FP	FeKa	290.647	0.437
O	35.6950 %	Quant.-FP	O Ka	0.355	0.052
Ca	6.7614 %	Quant.-FP	CaKa	52.363	0.205
Si	4.1807 %	Quant.-FP	SiKa	9.029	0.058
P	3.0956 %	Quant.-FP	P Ka	16.667	0.224
Mn	1.4444 %	Quant.-FP	MnKa	7.358	0.166
F	0.3669 %	Quant.-FP	F Ka	0.008	0.009
Ba	0.2771 %	Quant.-FP	BaLa	0.187	0.038
Al	0.2371 %	Quant.-FP	AlKa	0.551	0.037
Mg	0.1627 %	Quant.-FP	MgKa	0.114	0.016
Sr	0.0896 %	Quant.-FP	SrKa	0.897	0.229
C	0.0866 %	Quant.-FP	C Ka	0.655	0.093
K	0.0821 %	Quant.-FP	K Ka	0.678	0.112
S	0.0720 %	Quant.-FP	S Ka	0.338	0.072
Zn	0.0454 %	Quant.-FP	ZnKa	0.191	0.072
Na	0.0444 %	Quant.-FP	NaKa	0.011	0.007
Cr	0.0247 %	Quant.-FP	CrKa	0.126	0.102

XRF data show that the IRP used in this study is a powder with a high concentration of iron (47.33 %). The concentrations of other elements are in good agreement with their respective Clarke numbers in the Earth's crust,[S13] and the deviations from these factors may be related to the geochemical characteristics of the terrain from which the IRP was collected.

The XRD pattern evidenced, that IRP is amorphous to X-rays.

In the FTIR spectrum, two broad bands centered at ~478 and 983 cm^{-1} and two shoulder peaks at ~690 and 841 cm^{-1} are observed (**Fig. S1**). We believe that the spectrum, recorded in the range 400–1000 cm^{-1}, is a superposition of the spectra of goethite (α-FeOOH, making the greatest contribution to the peaks at 478 and 983 cm^{-1}), akaganeite (β-FeOOH, peaks at 690 and 841 cm^{-1}), and lepidocrocite (γ-FeOOH), which are the main polymorphic iron oxyhydroxide phases that occur in nature.[S14] Also, the pattern is well consistent with that obtained for a sample of "synthetic amorphous FeOOH."[S14]

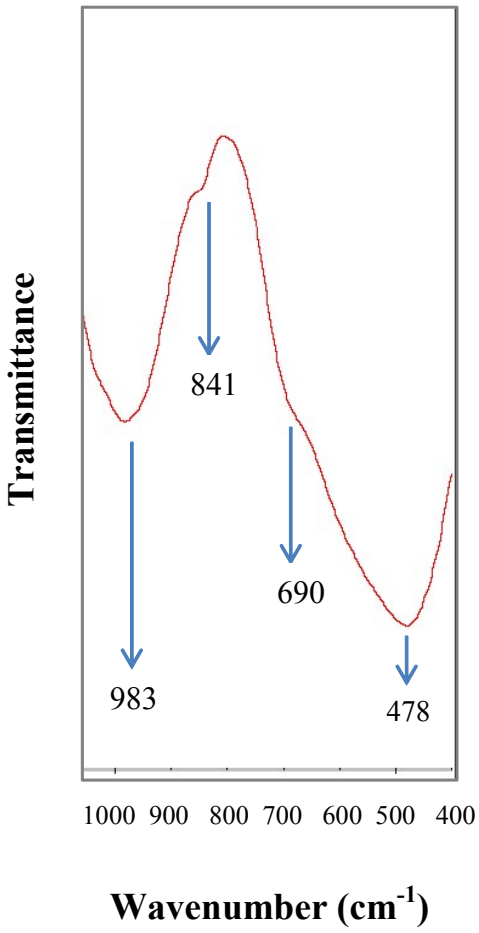

Figure S1. FTIR spectrum of IRP in the wavelength range of 400–1000 cm^{-1}.

The thermal analysis results obtained earlier showed that the initial IRP sample contains ~21.5 wt % adsorbed water.[S15]

Thus, the XRF, XRD, FTIR, and thermal analysis data collectively show that the IRP starting material (precursor) is a powder based, primarily, on amorphous iron hydroxides containing a rather large amount of water. Being a sediment obtained by deironing natural underground water, iron removal precipitate is naturally represented, besides iron and oxygen, by other elements more or less common in the Earth's crust. Among them are silicon, calcium, phosphorus, manganese (4.18, 6.76, 3.09, and 1.44 %, respectively), barium, aluminum, magnesium, and some other elements (in the amount of fractions of a percent) (**Table S1**). It is possible that impurities based on these elements can affect the

grain growth. For example, the possible positive role of SiO_2, which is capable of inhibiting the growth of particles,[S16] has been already mentioned in our previous work.

3.3. Characterization of prepared HNPCs

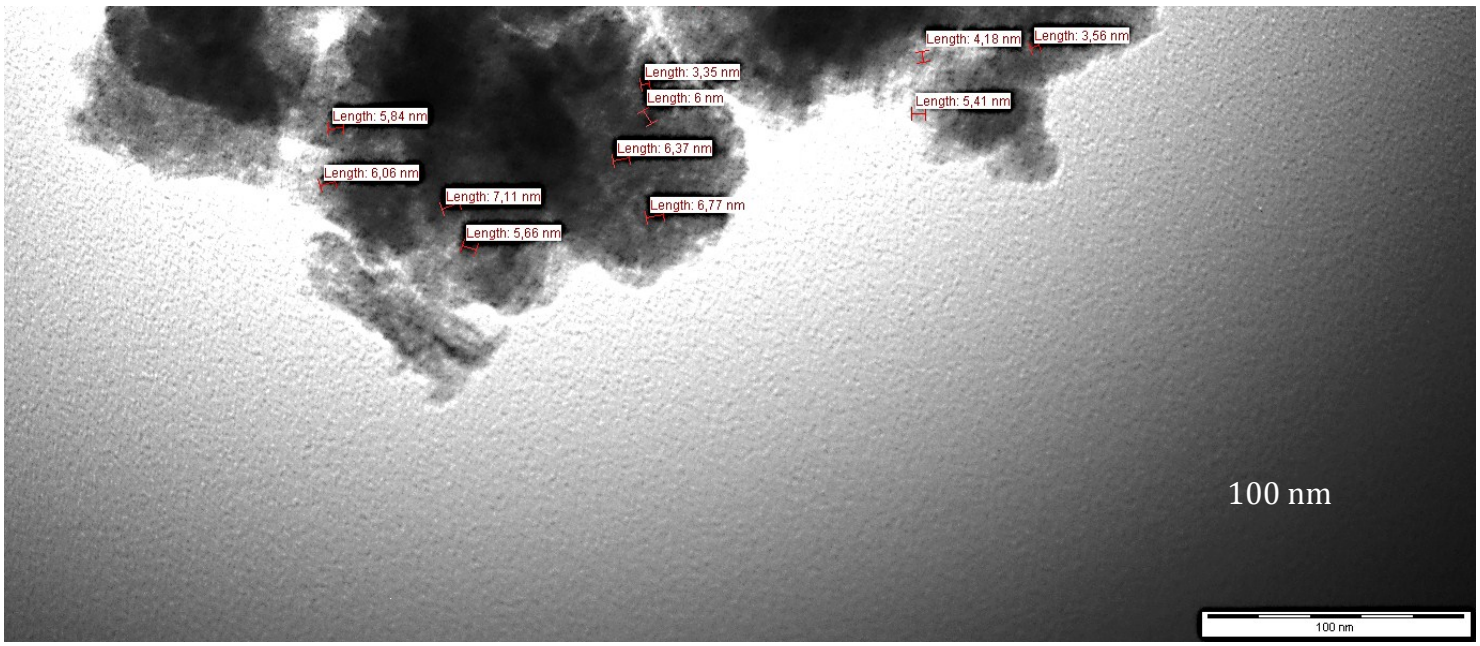

Figure S2. TEM image of HNPCs.

The emergence of secondary nanostructures is well consistent with a two-stage model of particle growth, according to which primary nanoparticles nucleate first and then aggregate into larger secondary structures.[S17–S18]

XRF data (**Table S2**) indicate that the final product of HNPCs inherited its elemental composition from the IRP precursor.

Table S2. Elemental composition of HNPCs

[Quantitative Result]

Analyte	Result	Proc-Calc	Line	Net Int.	BG Int.
Fe	42.8139 %	Quant.-FP	FeKa	282.315	0.434
O	41.2480 %	Quant.-FP	O Ka	0.430	0.054
Ca	6.3382 %	Quant.-FP	CaKa	51.268	0.239
Si	4.1571 %	Quant.-FP	SiKa	9.405	0.048
P	3.0590 %	Quant.-FP	P Ka	17.204	0.261
Mn	1.2069 %	Quant.-FP	MnKa	6.562	0.156
Al	0.3243 %	Quant.-FP	AlKa	0.790	0.055
Ba	0.2730 %	Quant.-FP	BaLa	0.193	0.035
Mg	0.1839 %	Quant.-FP	MgKa	0.135	0.021
C	0.0929 %	Quant.-FP	C Ka	0.726	0.099
S	0.0827 %	Quant.-FP	S Ka	0.404	0.074
K	0.0821 %	Quant.-FP	K Ka	0.707	0.119
Sr	0.0818 %	Quant.-FP	SrKa	0.903	0.209
Zn	0.0301 %	Quant.-FP	ZnKa	0.139	0.076
Cr	0.0261 %	Quant.-FP	CrKa	0.141	0.096

Thus, the combined TEM, FTIR, and Raman data clearly demonstrate that hematite nanoparticle clusters were obtained in the present study (see the main article). In terms of chemical composition, the magnetic properties of HNPCs are controlled by the presence of such a chemical element as iron. In our opinion, there are no impurities in HNPCs that can take on this crucial role. On the other hand, we can assume that the absence of such elements common in the Earth's crust as silicon, calcium, and others in the chemical composition of HNPCs could lead to some changes in the magnetic properties of this material, for example, an increase in the magnetization value.

3.4.

Table S3. Hematite nanomaterials demonstrating the high magnetization: Synthesis, chemical constituents and magnetization value

Hematite nanomaterial	Synthesis	Magnetiza-tion, emu g^{-1}	Chemical constituents, at %	Refe-rence	Notes: (i) Renewable source Fe^x or not/ (ii) Demands support or not
Nanoparticles α-Fe_2O_3-MCM[1]	Microwave combustion method (MCM)	65.2 (RT[2])	Fe - 46.40, O – 53.60[3]	S19[6]	(i) Unrenewable source Fe^x: $Fe(NO_3)_3{\cdot}9H_2O$; (ii) $CO(NH_2)_2$ as fuel and as reducing reactant.
Hematite nanorods	Pulse galvanostatic synthesis in the presence of external magnetic fields _ Calcination (400ºC, 2h)	85.0 (RT)	N/A[4]	S20	(i) Unrenewable source Fe^x: $FeSO_4$; (ii) $AgNO_3$ as nucleation starter.
Combustion-derived ultrasmall α-Fe_2O_3 nanoparticles	Combustion approach with template-assisted synthesis	21.0 (300 K)	N/A[4]	S21	(i) Unrenewable source Fe^x: $Fe(NO_3)_3{\cdot}9H_2O$; (ii) NH_4NO_3 as oxidizer, $C_2H_5NO_2$ as a "fuel", SBA-15 as a template.
Hematite nanoparticle clusters	"Sharp high-temperature dehydration"	51.0 (300 K)	Fe - 42.81, O – 41.24, Si – 4.15, Ca – 6.33, P – 3.05, Mn - 1.20[5]	This work	(i) Renewable source Fe^x _ Waste material; (ii) Without any support.

[1] MCM - microwave combustion method.

[2] RT – room temperature.

[3] EDX analysis data.

[4] The articles do not contain data on chemical analysis of final products.

[5] Elements with a concentration exceeding 1 % (Table S2, ESI); XRF data.

[6] Based on the chemical composition of the reagents used in S19-S21, it can be assumed that the synthesis of hematite nanomaterials is accompanied by the formation of by-products (primarily gaseous) in them, that are harmful to humans and the environment (for example, nitrogen oxides, ammonia, etc.). In addition, nonrenewable sources of Fe^x are used in these works.

4. SYNTHESIS OF HNPCs: ESSENTIAL DETAILS

Let us consider the major points of the formation of the HNPCs from the IRP. As shown above (**Section 3.2**), water is present in the IRP in both bound (as a part of oxyhydroxide phases) and free (physically adsorbed) forms. Upon treatment of the IRP with the gas burner flame (**Section 2.2**), a sharp, almost instantaneous evaporation of water takes place, which strips the water out of the material and practically disintegrates the particles of the initial powder at different hierarchical levels. The latter, apparently, contributes to the decrease in the sizes of the resulting particles and enhances their defect structure. At the same time, oxygen entering the open tube from the air contributes to the synthesis of the most thermodynamically stable form of iron oxide, i.e., hematite. We refer to this synthesis as "sharp high-temperature dehydration (SHTDH)."

The key factors of the SHTDH are the (i) very sharp, high-temperature and (ii) short exposure of the (iii) amorphous iron oxyhydroxide phases (the Fe^{3+} ion source) that contain a considerable amount of adsorbed water (iv) in an oxidizing atmosphere. These factors are considered in greater detail as follows.

(i) The sharp high-temperature exposure involves no preheating of the initial material prior to the treatment. The material is exposed to a high temperature immediately.

(ii) The short exposure means that there is no maintaining the product at an elevated temperature. Such a holding period could lead to the gradual

recrystallization of the synthesized particles, accompanied by an increase in their size and a change in their properties.

(iii) The amorphous iron oxyhydroxide phases considered here contain a significant amount of adsorbed water. They are produced as precipitates in the deironing of groundwater and should be the renewable Fe^{3+} ion source available around the world. It is expected, however, that synthetic iron hydroxides could also be used as a starting material for the synthesis of hematite nanoparticle clusters.

(iv) An oxidizing atmosphere is a medium with access to atmospheric oxygen (or other oxidizing agents).

Among the advantages of this synthesis are that it is rapid, one-stage, and environmentally friendly without templates, catalysts, or surfactants, and it does not involve a large number of reagents (including toxic and/or expensive materials).

The described synthesis of HNPCs by SHTDH can be viewed, on the one hand, as a version of the thermal decomposition of iron precursors. However, it most likely could serve as a starting point for developing a new approach to producing iron oxide-based nanomaterials. It should be noted that this approach agrees well with the principles of "green chemistry."

This approach could also be extended to the synthesis of nanomaterials with other compositions. By this sharp high-temperature exposure of appropriate precursors in open or closed systems (or systems with a preset atmosphere containing substances necessary for synthesizing a desired compound), various nanomaterials could be obtained. However, such studies have not been conducted to date, and could be the subject of future research.

CONFLICTS OF INTEREST

There are no conflicts to declare.

ACKNOWLEDGEMENTS

The author expresses gratitude to Yu.P. Pinzhin, E.P. Naiden, and S.A. Yushchenko (Tomsk Regional Common Use Center) for fruitful cooperation. The author is grateful to B. Budaev and D.A. Kryuchkov (Termex Company, Tomsk) for their help in this work. The author is also grateful to the Joint-use Center of Tomsk Scientific Center of SB RAS for providing access to the Nicolet 5700 FTIR spectrometer, and N.V. Ryabova (Institute of Petroleum Chemistry, SB RAS) for recording IR spectra. The author also thanks the anonymous referees for their useful comments.

REFERENCES

S1 W. Stumm and G. F. Lee, *Ind. Eng. Chem.*, 1961, **53**, 143.

S2 S. Chaturvedi and P. N. Dave, *Desalination*, 2012, **303,** 1.

S3 I. A. Katsoyiannis and A. I. Zouboulis, *Water Res*., 2004, **38**, 1922.

S4 R. Munter, H. Ojaste and J. Sutt, *J. Environ. Eng. Div. (Am. Soc. Civ. Eng.)*, 2005, **131**, 1014.

S5 S. L. Shvartsev and O. V. Kolokolova, *Proceedings of the 2003 International Symposium on Water Resources and the Urban Environment* (Wuhan, China, 9-10 November 2003), 2003, 353.

S6 I. S. Ivanova, O. E. Lepokurova, O. S. Pokrovsky and S. L. Shvartsev, *Procedia Earth and Plantetary Science,* 2013, **7**, 385.

S7 E. E. Sirotkina and L. Yu. Novoselova, *Chem. Technol. Fuels Oils*, 2007, **43**, 395.

S8 (a) L. Yu. Novoselova, E. E. Sirotkina and N. I. Pogadaeva, *Pet. Chem.,* 2008, **48**, 67; (b) L. Yu. Novoselova and E. E. Sirotkina, *Russ. J. Phys. Chem. A*, 2010, **84**, 1033; (c) L. Yu. Novoselova, *Powder Technol.,* 2013, **243**, 149**.**

S9 A. Hamdouni, G. Montes-Hernandez, M. Tlili, N. Findling, F. Renard and C. V. Putnis, *Chem. Eng. J.*, 2016, **283**, 404.

S10 P. Anastas and N. Eghbali, *Chem. Soc. Rev*., 2010, **39**, 301.

S11 D. L. A. deFaria, S. V. Silva and M. T. deOliveira, *J. Raman Spectrosc*., 1997, **28**, 873

S12 V. Yu. Kreslin and E. P. Naiden, *Instrum. Exp. Tech*., 2002, **45**, 55.

S13 (a) S. R. Taylor, *Geochim. Cosmochim. Acta*, 1964, **28**, 1273; (b) P. A. Cox, *The Elements: Their Origin, Abundance, and Distribution*, Oxford University Press, Oxford, 1989.

S14 W. Sung and J. J. Morgan, *Environ. Sci. Technol*., 1980, **14**, 561.

S15 L. Yu. Novoselova and E. E. Sirotkina, *Russ. J. Phys. Chem. A,* 2009, **83**, 2127.

S16 L. Yu. Novoselova, *Powder Technol.*, 2016, **287**, 364.

S17 (a) J. P. Ge, Y. X. Hu, M. Biasini, W. P. Beyermann and Y. D. Yin, *Angew. Chem., Int. Ed.,* 2007, **46**, 4342; (b) L. S. Zhong, J. S. Hu, H. P. Liang, A. M. Cao, W. G. Song and L. J. Wan, *Adv. Mater.*, 2006, **18**, 2426.

S18 (a) H. M. Zheng, R. K. Smith, Y. W. Jun, C. Kisielowski, U. Dahmen and A. P. Alivisatos, *Science*, 2009, **324**, 1309; (b) C. J. Johnson, E. Dujardin, S. A. Davis, C. J. Murphy and S. Mann, *J. Mater. Chem.,* 2002, **12**, 1765.

S19 A. Manikandan, J. J. Vijaya and L. J. Kennedy, *J. Nanosci. Nanotechnol*., 2013, **13**, 2986.

S20 H. Karami, J. Ordoukhanian and A. Nezhadali, *Ceram. Int*., 2015, **41**, 14760.

S21 K.V. Manukyan, Y.S. Chen, S. Rouvimov, P. Li, X. Li, S.N. Dong, X.Y. Liu, J.K. Furduna, A. Orlov, G.H. Bernstein, W. Porod, S. Roslyakov and A.S. Mukasyan, *J. Phys. Chem. C*, 2014, **118,** 16264.